Electronic Spectra and Photophysics of Platinum(II) Complexes with α-Diimine Ligands. Mixed Complexes with Halide Ligands

Vincent M. Miskowski,*[1a] Virginia H. Houlding,*[1b] Chi-Ming Che,*[1c,d] and Yu Wang[1d]

Arthur Amos Noyes Laboratory,† California Institute of Technology, Pasadena, California 91125, Bandgap Technology Corporation, Broomfield, Colorado 80021, Department of Chemistry, The University of Hong Kong, Pokfulam Road, Hong Kong, and Department of Chemistry, National Taiwan University, Taipei, Taiwan

Received September 10, 1992

Emission properties have been studied for a series of compounds of the formula $(L_2)PtCl_2$, where L_2 is *N,N,N',N'*-tetramethylethylenediamine, 2,2'-bipyridine (bpy), 4,4'-Me_2bpy, 5,5'-Me_2bpy, 4,4'-$(t\text{-Bu})_2$bpy, 3,3'-$(CH_3OCO)_2$bpy, and 1,10-phenanthroline, and also for the compound $Pt(bpy)I_2$. Most of them exhibit orange to red luminescence from a triplet ligand-field (^{3}LF) state, both as solids and in glassy solution. These emissions are very broad (fwhm 2300–3400 cm^{-1} at 10 K) and structureless and are strongly Stokes-shifted from absorption. The two exceptions are the solid "red" form of $Pt(bpy)Cl_2$, which exhibits a relatively narrow (fwhm 1050 cm^{-1} at 10 K), vibronically structured ($\Delta\nu \sim 1500$ cm^{-1}) red emission, and $Pt(3,3'\text{-}(CH_3OCO)_2bpy)Cl_2$, which exhibits a broad (fwhm 2500 cm^{-1} at 10 K) but structured ($\Delta\nu \sim 1300$ cm^{-1}) orange emission. Both of these emissions are assigned to triplet metal-to-ligand charge-transfer (^{3}MLCT) excited states. For the former compound, a linear-chain structure has destabilized a $d\sigma^*(d_{z^2})$ level, yielding a $d\sigma^* \rightarrow \pi^*$(bpy) state as the lowest energy excited state, while for the latter, the strongly electron-withdrawing substituents have stabilized a bpy π^* level, yielding a $d_{xz,yz} \rightarrow \pi^*$(bpy) state as the lowest energy excited state. The relative energies of the various types of excited states, including ligand $3\pi\pi^*$ states, are discussed in detail. The crystal structures of $Pt(5,5'\text{-}Me_2bpy)Cl_2$ (monoclinic *Cc*, $Z = 4$, $a = 13.413(7)$ Å, $b = 9.063(4)$ Å, $c = 12.261(9)$ Å, $\beta = 121.71(6)°$) and $Pt(3,3'\text{-}(CH_3OCO)_2bpy)Cl_2$ (triclinic $P\bar{1}$, $Z = 2$, $a = 7.288(2)$ Å, $b = 9.932(3)$ Å, $c = 11.881(5)$ Å, $\alpha = 98.04(3)°$, $\beta = 103.56(3)°$, $\gamma = 106.54(3)°$) are reported.

For a number of years, we have been interested in the electronic structure of Pt(II) α-diimine complexes. Crystalline structure can have a pronounced effect on the lowest electronic states of these complexes, which we have probed via diffuse reflectance, luminescence, and excited-state-lifetime measurements. Our studies[2] have revealed a remarkable variety of lowest energy excited triplet states. These include α-diimine intraligand (IL) states of both monomer (π–π^*) type and "excimer" (π–π^*) type, oligomer metal-to-ligand charge-transfer (MLCT) states involving metal–metal-perturbed triplet $d\sigma^*(d_{z^2}) \rightarrow \pi^*$(α-diimine) excitation, and simple monomer ligand-field (LF) states. In the case of strong-field complexes,[2b] we have documented how strong Pt–Pt electronic interaction in e.g. a linear-chain structure can result in a change in the lowest excited state from ^{3}IL to ^{3}MLCT. In this paper, we explore the electronic structure and solid-state effects in a series of weaker field complexes of the type Pt(diimine)X_2 where X is chloride or iodide.

In our initial work,[2a] we used the compound $Pt(bpy)Cl_2$ (bpy = 2,2'-bipyridine) as our example of ^{3}LF emission. While the results presented in ref 2a, including both solid-state and glassy-solution emission, as well as excitation spectra, were conclusively in favor of our interpretation, further work seemed called for both because of a puzzling disagreement of our observations in glassy solution with those of the literature[3] and because of our initial studies of closely related compounds such as $Pt(phen)Cl_2$ (phen = 1,10-phenanthroline) giving broadly vibronically structured (frequency intervals of 1000–1500 cm^{-1}) emission spectra that seemed to be incompatible with a ^{3}LF assignment. In the end, both of these problems had a common solution: the Pt(α-diimine)X_2 (X = halide) compounds are very poorly soluble in common solvents and are prone to contamination with highly luminescent impurities.[4] The *pure* materials of this type yield emissions that are unequivocally ^{3}LF, as shown in this paper.

The compound $Pt(bpy)Cl_2$ crystallizes as two different polymorphs, a yellow form with no significant Pt–Pt interaction (d(Pt–Pt) = 4.5 Å)[5a] and a red form having linear chains and a Pt–Pt distance of 3.45 Å.[5] We have now found that the emissions of the two forms are completely distinctive, despite coincidental similarity of their emission maxima at room temperature. We present evidence for a changeover of lowest energy excited states from ^{3}LF (yellow form) to oligomer ^{3}MLCT (linear-chain red form), and we present one example of an emissive monomer with a lowest energy ^{3}MLCT state derived from $d\pi \rightarrow \pi^*$(α-diimine), a class not represented in any of our previous studies.

Experimental Section

Preparation of Compounds. All compounds reported analyzed well (C, H, N) for the indicated formulations.

The compound $Pt(tmen)Cl_2$ (**1**; tmen = *N,N,N',N'*-tetramethylethylenediamine) was prepared by adding a 50% excess of tmen to a clear yellow solution of *cis*-$Pt(CH_3CN)_2Cl_2$ (Aldrich) in the minimum volume of CH_3CN held at about 70 °C. After 1.5 h of stirring, a light yellow precipitate had formed. Cooling to room temperature, filtration, washing with ether, and air-drying yielded **1** in 70% yield.[6] This procedure is simpler than those of ref 7.

† Contribution No. 8719.

(1) (a) California Institute of Technology. (b) Bandgap Technology Corp. (c) The University of Hong Kong. (d) National Taiwan University.

(2) (a) Miskowski, V. M.; Houlding, V. H. *Inorg. Chem.* **1989**, *28*, 1529. (b) Miskowski, V. M.; Houlding, V. H. *Inorg. Chem.* **1991**, *30*, 4446. (c) Houlding, V. H.; Miskowski, V. M. *Coord. Chem. Rev.* **1991**, *111*, 145. (d) Wan, K.-T.; Che, C.-M.; Cho, K.-C. *J. Chem. Soc., Dalton Trans.* **1991**, 1077. (e) Che, C.-M.; Wan, C. M.; He, L.-Y.; Poon, C. K.; Yam, Y. W. W. *J. Chem. Soc., Chem. Commun.* **1989**, 2011.

(3) Webb, D. L.; Rossiello, L. A. *Inorg. Chem.* **1971**, *10*, 2213.

(4) On the basis of preliminary studies (W. B. Connick and H. B. Gray, private communication), aqua/hydroxo complexes appear to be the most tenacious strongly emissive impurities. Free α-diimine, protonated α-diimine, and Pt(α-diimine)$_2^{2+}$ may also appear as impurities in crude materials.

(5) (a) Textor, V. M.; Oswald, H. R. *Z. Anorg. Allg. Chem.* **1974**, *407*, 244. (b) Osborn, R. S.; Rogers, D. *J. Chem. Soc., Dalton Trans.* **1974**, 1002.

(6) Additional material may be obtained by addition of ether to the filtrate, but it is greenish in color and clearly impure. We did not make any attempt to purify it.

0020-1669/93/1332-2518$04.00/0

Table I. Crystallographic Data for Pt(5,5′-Me_2bpy)Cl_2 (**6**) and Pt(33′-$(CH_3OCO)_2$bpy)Cl_2 (**8**)

	6	**8**
formula	$PtCl_{12}H_{12}H_2Cl_2$	$PtC_{14}H_{12}N_2O_4Cl_2$
fw	450.23	538.19
space grp	*Cc*	$P\bar{1}$
a, Å	13.413(7)	7.288(2)
b/Å	9.063(4)	9.932(3)
c/Å	12.261(9)	11.881(5)
α/deg	90	98.04(3)
β/deg	121.71(6)	103.56(3)
γ/deg	90	106.54(3)
V/Å^3	1268.0(1)	781.5(5)
Z	4	2
F(000)/electrons	840	508
T/°C	25	25
λ/Å	0.710 69	0.710 69
D_{calc}/g cm^{-3}	2.358	2.249
μ/cm^{-1}	0.49–1.0	0.54–1.0
R^a	0.035	0.032
$R_w{}^b$	0.031	0.034

^{a} $R = \sum||F_o| - |F_c||/\sum F_o$. ^{b} $R_w = (\sum w(F_o - |F_c|)^2/\sum wF_o^2)^{1/2}$.

The compounds Pt(4,4′-Me_2bpy)Cl_2 (**2**), Pt(4,4′-(*t*-Bu)$_2$bpy)Cl_2 (**3**), Pt(phen)Cl_2 (**4**), yellow Pt(bpy)Cl_2 (**5a**), Pt(5,5′-Me_2bpy)Cl_2 (**6**), and Pt(3,3′-$(CH_3OCO)_2$bpy)Cl_2 (**8**) were all prepared by the method of Morgan and Burstall,[8] as modified by others.[9] The rather insoluble **4** and **5a** contained luminescent impurities as prepared but could be purified by slow cooling of hot saturated solutions in dimethylformamide (DMF) to yield yellow needles with reproducible emission spectra and photophysical properties. The red form of Pt(bpy)Cl_2 (**5b**) was prepared as described.[9a]

Pt(bpy)I_2 (**7**) was prepared as described[10] and further purified by recrystallization from hot DMF to yield orange needles.

Photophysical Measurements. Most of our equipment has been previously described.[2] The solid-state emission spectra reported here were recorded on a new system, a Spex Ramalog Raman spectrometer consisting of a Spectra Physics 2020 5-W argon ion laser, a Spex 1404 double 1-m monochromater, and an RCA C31034M single-photon-counting detector. The 457.9-nm laser line was used unless otherwise noted. Incident intensity was reduced to the range 2–200 μW/cm^2 by means of neutral-density filters. Low-temperature measurements were performed on powder samples held in sealed quartz capillaries mounted in a CTI 350CP closed-cycle He refrigerator from Janis Research.

X-ray Crystallography. Pt(5,5′-Me_2bpy)Cl_2. A yellow crystal of dimensions 0.20 × 0.35 × 0.30 mm was mounted on a glass fiber on an Enraf-Nonius CAD-4 diffractometer. Cell dimensions and space group (see Table I) were determined from refinement of 25 reflections with a 2θ range of 21.38–31.34°. Intensity data were collected with a θ/2θ scan at a variable scan speed of 1.3–8.2°/min. A total of 1507 unique reflections were collected, of which 1338 had $I_{net} \geq 2.0\sigma(I_{net})$ and were considered to be observed. Three standard reflections were checked every 60 min; intensity variations were less than 3%. An empirical absorption correction was applied.

Pt(3,3′-$(CH_3OCO)_2$bpy)Cl_2. A clear yellow crystal of dimensions 0.30 × 0.50 × 0.50 mm was mounted on a glass fiber on an Enraf-Nonius CAD-4 diffractometer. Cell dimensions and space group (see Table I) were determined from refinement of 25 reflections with a 2θ range of 21.62–27.78°. Intensity data were collected with a θ/2θ scan at a variable scan speed of 1.5–8.2°/min. A total of 2991 reflections were collected, of which 2753 were unique, and 2566 of these had $I_{net} \geq 2.0\sigma(I_{net})$ and were considered to be observed. Three standard reflections were checked every 60 min; intensity variations were less than 4%. An empirical absorption correction was applied.

Structure Refinements. The platinum and chlorine atoms of both structures were located by MULTAN 82, and all of the other atoms were located from subsequent Fourier difference syntheses. Refinement was performed by full-matrix least-squares procedures, minimizing the function $\sum w(F_o - |F_c|)$, where $w = 1/\sigma^2(F_o)$. The hydrogen atoms were located but not refined. Secondary extinction parameters were refined in both cases; final values were 0.27(1) × 10^{-4} and 1.17(3) × 10^{-4} for **6** and **8**, respectively. The final difference maps showed maximum excursions of 2.47 and −1.80 e Å^3 for **6** and 1.29 and −2.09 e Å^3 for **8**. Bond distances and angles are included in Tables II and III.

Table II. Selected Bond Distances and Bond Angles of Compound **6**

	Distances (Å)		
Pt–Cl(1)	2.279(4)	C(2)–C(11)	1.56(2)
Pt–Cl(2)	2.311(4)	C(3)–C(4)	1.37(2)
Pt–N(1)	2.02(1)	C(4)–C(5)	1.36(2)
Pt–N(2)	2.01(1)	C(5)–C(6)	1.43(2)
N(1)–C(1)	1.36(2)	C(6)–C(7)	1.37(2)
N(1)–C(5)	1.36(2)	C(7)–C(8)	1.48(3)
N(2)–C(6)	1.37(2)	C(8)–C(9)	1.33(3)
N(2)–C(10)	1.38(2)	C(9)–C(10)	1.36(2)
C(1)–C(2)	1.39(2)	C(9)–C(12)	1.49(2)
C(2)–C(3)	1.40(3)		
	Angles (deg)		
Cl(1)–Pt–Cl(2)	89.8(2)	C(3)–C(2)–C(11)	125(2)
Cl(1)–Pt–N(1)	96.0(4)	C(2)–C(3)–C(4)	118(2)
Cl(1)–Pt–N(2)	175.2(3)	C(3)–C(4)–C(5)	124(2)
Cl(2)–Pt–N(1)	171.7(4)	N(1)–C(5)–C(4)	117(1)
Cl(2)–Pt–N(2)	93.9(3)	N(1)–C(5)–C(6)	113(1)
N(1)–Pt–N(2)	80.1(5)	C(4)–C(5)–C(6)	130(2)
Pt–N(1)–C(1)	123(1)	N(2)–C(6)–C(5)	117(1)
Pt–N(1)–C(5)	116(1)	N(2)–C(6)–C(7)	125(1)
C(1)–N(1)–C(5)	121(1)	C(5)–C(6)–C(7)	118(1)
Pt–N(2)–C(6)	113.7(9)	C(6)–C(7)–C(8)	111(2)
Pt–N(2)–C(10)	128(1)	C(7)–C(8)–C(9)	125(2)
C(6)–N(2)–C(10)	118(1)	C(8)–C(9)–C(10)	118(2)
N(1)–C(1)–C(2)	121(2)	C(8)–C(9)–C(12)	122(2)
C(1)–C(2)–C(3)	118(2)	C(10)–C(9)–C(12)	121(2)
C(1)–C(2)–C(11)	117(2)	N(2)–C(10)–C(9)	122(2)

Table III. Selected Bond Distances and Bond Angles of Compound **8**

	Distances (Å)		
Pt–Cl(1)	2.287(2)	C(5)–C(10)	1.49(1)
Pt–Cl(2)	2.282(3)	C(6)–C(7)	1.37(1)
Pt–N(1)	2.004(7)	C(7)–C(8)	1.39(1)
Pt–N(2)	1.979(7)	C(8)–C(9)	1.36(1)
N(1)–C(1)	1.335(10)	C(9)–C(10)	1.40(1)
N(1)–C(5)	1.363(10)	C(9)–C(13)	1.49(1)
N(2)–C(6)	1.372(10)	C(11)–O(11)	1.21(1)
N(2)–C(10)	1.365(10)	C(11)–O(2)	1.33(1)
C(1)–C(2)	1.397(12)	C(12)–O(2)	1.50(1)
C(2)–C(3)	1.363(13)	C(13)–O(3)	1.21(1)
C(3)–C(4)	1.389(11)	C(13)–O(4)	1.32(1)
C(4)–C(5)	1.392(11)	C(14)–O(14)	1.43(1)
C(4)–C(11)	1.477(12)		
	Angles (deg)		
Cl(1)–Pt–Cl(2)	88.81(9)	N(1)–C(5)–C(10)	113.1(7)
Cl(1)–Pt–N(1)	95.6(2)	C(4)–C(5)–C(10)	127.9(7)
Cl(1)–Pt–N(2)	174.5(2)	N(2)–C(6)–C(7)	122.0(7)
Cl(2)–Pt–N(1)	173.9(2)	C(6)–C(7)–C(8)	119.2(7)
Cl(2)–Pt–N(2)	96.0(2)	C(7)–C(8)–C(9)	119.5(7)
N(1)–Pt–N(2)	79.7(3)	C(8)–C(9)–C(10)	120.3(8)
Pt–N(1)–C(1)	123.2(6)	C(8)–C(9)–C(13)	114.7(7)
Pt–N(1)–C(5)	114.6(5)	C(10)–C(9)–C(13)	124.8(7)
C(1)–N(1)–C(5)	121.0(7)	N(2)–C(10)–C(5)	110.9(7)
Pt–N(2)–C(6)	123.8(6)	N(2)–C(10)–C(9)	120.2(7)
Pt–N(2)–C(10)	117.6(5)	C(5)–C(10)–C(9)	128.7(7)
C(6)–N(2)–C(10)	118.2(7)	C(4)–C(11)–O(1)	124.1(8)
N(1)–C(1)–C(2)	120.7(8)	C(4)–C(11)–O(2)	111.6(7)
C(1)–C(2)–C(3)	118.9(8)	O(1)–C(11)–O(2)	124.3(8)
C(2)–C(3)–C(4)	119.9(8)	C(9)–C(13)–O(3)	122.3(8)
C(3)–C(4)–C(5)	119.2(8)	C(9)–C(13)–O(14)	114.9(6)
C(3)–C(4)–C(11)	117.8(7)	O(3)–C(13)–O(4)	122.6(8)
C(5)–C(4)–C(11)	122.2(7)	C(11)–O(2)–C(12)	115.9(7)
N(1)–C(5)–C(4)	118.9(7)	C(13)–O(4)–C(14)	119.1(7)

Results and Discussion

Crystallographic Results. The molecular units found in the crystals of **6** and **8** are shown in Figures 1 and 2. The structures

(7) Mann, F. G.; Watson, H. R. *J. Chem. Soc.* **1958**, 2772.
(8) Morgan, G. T.; Burstall, F. H. *J. Chem. Soc.* **1934**, 965.
(9) (a) Bielli, E.; Gidney, P. M.; Gillard, R. D.; Heaton, B. T. *J. Chem. Soc., Dalton Trans.* **1974**, 2133. (b) Palocsay, F. A.; Rund, J. V. *Inorg. Chem.* **1969**, *8*, 524. (c) Dholakia, S.; Gillard, R. D.; Wimmer, S. L. *Polyhedron* **1985**, *4*, 791.
(10) Wimmer, S.; Castan, P.; Wimmer, F. L.; Johnson, N. P. *J. Chem. Soc., Dalton Trans.* **1989**, 403.

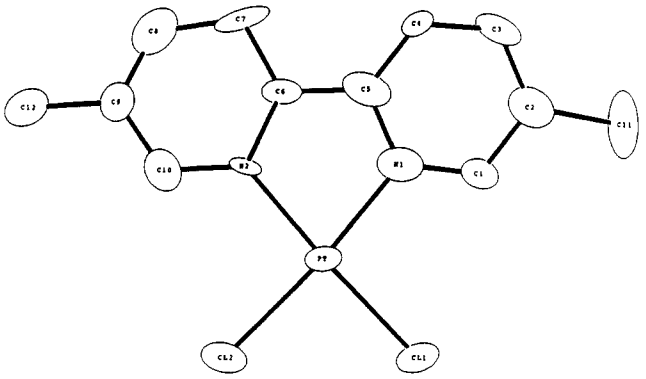

Figure 1. ORTEP drawing of the molecular unit of **6**.

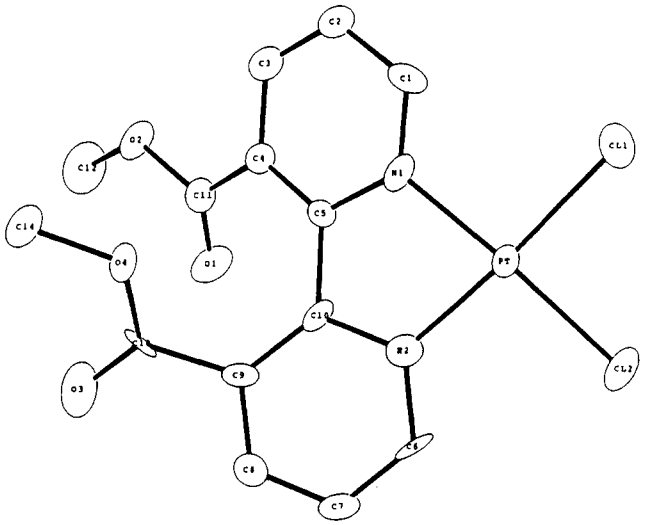

Figure 2. ORTEP drawing of the molecular unit of **8**.

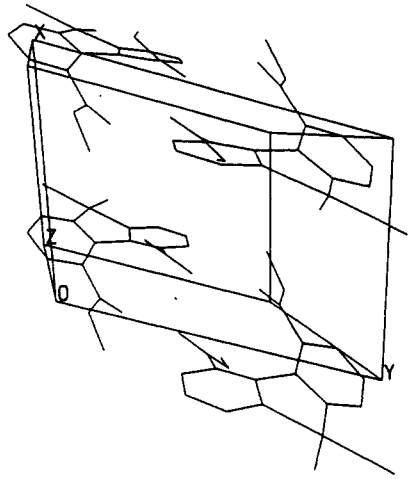

Figure 3. Unit cell contents for compound **8**.

are for the most part unremarkable, showing the expected planar *cis*-PtN_2Cl_2 core units. There are two noteworthy features.

First, the Pt–Cl bonds of **8** (2.285 Å average) are significantly shorter than those of **6** (2.345 Å average). A probable explanation of this effect is that 3,3′-$(CH_3OCO)_2$bpy is a better π-acceptor than 5,5′-Me_2bpy, which reduces $d\pi$ electron density on Pt so as to allow for stronger π-donation by Cl^- in **8**, hence shorter (stronger) Pt–Cl bonds.

Second, the substituted bpy ligand of **8** is markedly nonplanar, in contrast to that of **6**, as is more clearly shown in Figure 3. The dihedral angles between the average pyridyl planes of the bpy units are 25.5(3)° for **8** and 4.8(6)° for **6**. We believe that this reflects a compromise between maximum π-conjugation between the two pyridyl rings (planar bipyridine) and maximum π-conjugation of the carbomethoxy units with the pyridyl rings. Because of steric repulsion between the two carbomethoxy units, the entire molecule cannot be planar. The observed carbomethoxy–pyridyl dihedral angles of 26.1(7) and 25.5(3)° for the halves of the ligand would presumably have had to be considerably larger if the bipyridine unit were planar.

We were interested in whether any close Pt–Pt or ligand–ligand contacts would be found in these structures, since either type of contact can greatly perturb electronic emission spectra.[2] None were found. (See Figures 3 and S-1 (supplementary material).) The closest Pt–Pt contacts in the crystals of **6** and **8** are 6.318(6) and 4.791(2) Å, respectively, and bpy–bpy contacts are of similar magnitude.

Emission Results. The emission properties of the compounds are summarized in Table IV. Three distinct types of emission have been observed.

Ligand Field Emission. Compound **1** is taken as a standard for ligand-field (d–d) emission from the *cis*-$Pt^{II}N_2Cl_2$ chromophore.[11] The broad, Gaussian-shaped orange emission observed both for the solid and for the glassy solution (ethanol/methanol, 77 K) is similar to that of other square planar complexes such as $PtCl_4^{2-}$.[3,14] Because of the low symmetry, assignment to a specific ^{3}LF excited state seems unwarranted, although comparison to the literature[15] strongly suggests that one of the $d\pi(xy,xz,yz) \rightarrow x^2 - y^2$ excited states should lie lowest.

Compounds **2**, **3**, **4**, **5a**, and **6** all exhibit emission that is very similar to that of **1**, both as solids and from glassy (ethanol/methanol or butyronitrile) or frozen (DMF) solution. Figure 4 shows data for **2**, which are typical. At low temperature the emissions are narrower, but they exhibit very little shift in intensity maximum.[16] None of them exhibit any vibronic structure at 10 K.[19] Excitation spectra for 77 K glassy solutions of **5** were previously[2a] found to reproduce the absorption spectrum, and similar results have been obtained by us for **2** and **4**. Compound **5a** is known to have closest Pt–Pt contacts of 4.5 Å in the crystal,[5a] and **6** and **8** have been shown to have still longer contacts in this work. Most likely all of these yellow compounds have well-isolated monomers in the crystal.

A ^{3}LF assignment seems indicated for these emissions, and support is provided by the emission of **7**, which is considerably

(11) The compounds Pt(en)Cl_2 and *cis*-$Pt(NH_3)_2Cl_2$ might seem to be reasonable standards, but we find that pure crystalline samples of these compounds do not exhibit detectable emission, even at 10 K. Reference 12 reported similar observations for *cis*-$Pt(NH_3)_2Cl_2$; interestingly, this compound is reported to be luminescent in frozen solution. Both of these compounds crystallize in chain structures,[13] which may somehow be related to the absence of LF emission. The bulky tmen ligand of **1** should suppress metal–metal stacking.

(12) Patterson, H. H.; Tewksbury, J. C.; Martin, M.; Krogh-Jespersen, M.-B.; LoMenzo, J. A.; Hooper, H. O.; Viswanath, A. K. *Inorg. Chem.* **1981**, *20*, 2297.

(13) (a) Iball, J.; McDonough, M.; Scrimgeour, S. *Acta Crystallogr., Sect. B* **1975**, *B31*, 1672. (b) Milburn, G. H. W.; Truter, M. R. *J. Chem. Soc. A* **1966**, 1609.

(14) Yersin, H.; Otto, H.; Zink, J. H.; Gliemann, G. *J. Am. Chem. Soc.* **1980**, *102*, 951 and references cited therein.

(15) (a) Martin, D. S., Jr. In *Extended Linear Chain Compounds*; Miller, J. S., Ed.; Plenum Press: New York, 1982. (b) Van Quickenborne, L. G.; Ceulemans, A. *Inorg. Chem.* **1981**, *20*, 796.

(16) Band moment theory[17] explains the band narrowing as being due to the cooling out of the thermally excited low-frequency metal–ligand stretching and bending modes that are associated with the ^{3}LF excited-state distortion.[14] According to this theory, the thermal shift in the maximum of a Gaussian profile band should only be of the order of the average thermally accessible Franck–Condon-active vibrational frequency. "Anharmonic" effects (of which thermal lattice contraction along a metal–metal stacking axis is a drastic example) can result in much larger thermal shifts of the band maximum.[18]

(17) Markham, J. J. *Rev. Mod. Phys.* **1959**, *31*, 956.

(18) (a) Miskowski, V. M.; Smith, T. P.; Loehr, T. M.; Gray, H. B. *J. Am. Chem. Soc.* **1985**, *107*, 7925. (b) Gliemann, G.; Yersin, H. *Struct. Bonding* **1985**, *62*, 87.

(19) We were not able to verify a claim (Hoggard, P. E.; Albin, M. *Inorg. Chem.* **1981**, *20*, 4413) of weak vibronic structure in the emission of **5a** at 12 K.

Table IV. Photophysical Data for Microcrystalline Pt(II) Diimine Compounds[a]

		300 K			10 K			rel emission yield, 10 K/300 K	
no.	formula	ν_{max}/cm^{-1}	fwhm/cm^{-1}	τ/ns	ν_{max}/cm^{-1}	fwhm/cm^{-1}	τ/ns	ratio of lifetimes	ratio of intensities
1	$Pt(tmen)Cl_2$	15 500	4600	<20	16 000	3400	<20		25
2	$Pt(4,4'\text{-}Me_2bpy)Cl_2$	15 400	3900	3340	15 150	2900			6.9
3	$Pt(4,4'\text{-}t\text{-}Bu_2bpy)Cl_2$	15 500	3900	<20	15 500	2600	~50		250
4	$Pt(phen)Cl_2$	15 900	3700	2400	15 900	3000	13 300	5.5	12
5a	$Pt(bpy)Cl_2$ yellow form	15 600[b]	4000[b]	500[b]	15 800	2400	3500		
5b	$Pt(bpy)Cl_2$ red form	16 300	2020	250	15 370	1050	435	1.7	2.8
					13 750 sh				
6	$Pt(5,5'\text{-}Me_2bpy)Cl_2$	15 400	4000	1140	15 250	3400	5100	4.1	2.5
7	$Pt(bpy)I_2$	14 400	2650	5620	14 400	2300	30 700	5.5	3.0
8	$Pt(3,3'\text{-}(CH_3OCO)_2bpy)Cl_2$	18 000 sh	~2900	350	18 050	~2500	1100	3.1	2.4
		17 050			16 800				
		15 000 sh			15 500 sh				

[a] Emission spectra taken with 457.9-nm excitation; emission lifetimes taken with 355-nm 20-ns pulsed excitation and collected >550 nm; fwhm = full width at half-maximum. [b] Emission was too weak to measure at 300 K; values listed were measured at 250 K.

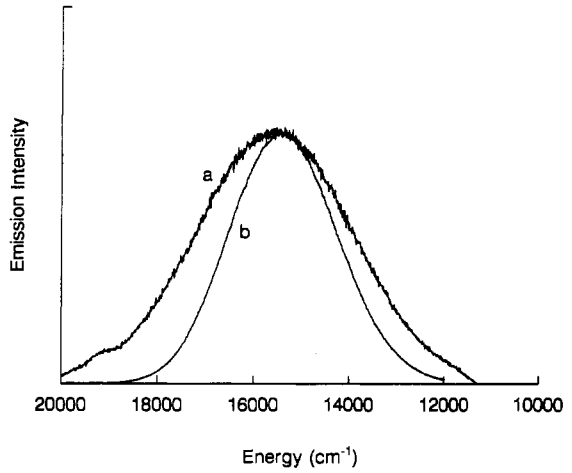

Figure 4. Emission spectra of solid **2** at 300 K (a) and 10 K (b). Excitation was at 457.9 nm, and the two spectra have been normalized to equal peak intensity.

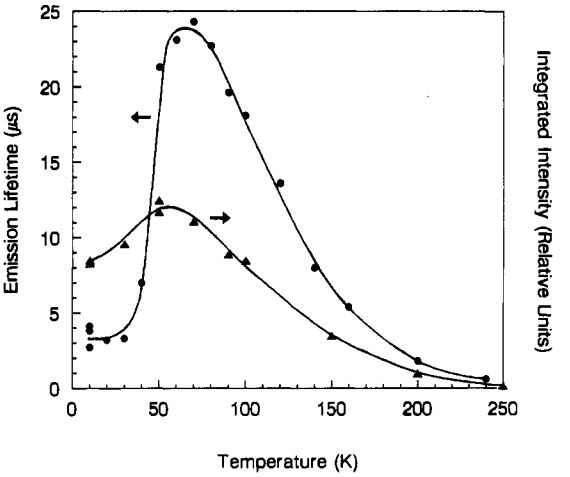

Figure 5. Dependence of emission lifetime τ (μs) and integrated intensity I (arbitrary units) upon temperature for solid **5a**. Excitation was at 457.9 nm for I measurements and at 355 nm for τ measurements.

red-shifted from that of **5a**, as expected for a ligand-field excited state of the *cis*-PtN_2I_2 chromophore.

The temperature dependences of the solid-state ^{3}LF emissions vary considerably among these compounds. Most fall into either of two categories. Compounds **2**, **4**, **6**, and **7** display strong long-lived emission even at 300 K, and emission lifetimes increase by a factor of about 5 at 10 K. Emission intensities are increased at 10 K by factors similar to those of the lifetimes; differences between the two ratios (Table IV) may possibly reflect a real temperature dependence of (average) radiative rate constants due to thermal population of a manifold of ^{3}LF spin–orbit components,[12,20] but we consider the intensity ratios to be subject to larger error owing both to the possibility of temperature-dependent changes in sample absorption and scattering and, more trivially, to sample alignment. We therefore do not attempt to quantitatively analyze these small temperature dependences. The lifetime of the emission of **4** was also determined at 77 K and found to be of intermediate magnitude, 8200 ns.

A second category is represented by **1** and **3**. These compounds exhibit extremely weak emission at 300 K; the intensity increases dramatically at lower temperature, but both intensity and lifetime are still very much less than those of the compounds of the first category. The strong temperature dependence suggests a thermally activated nonradiative decay process,[21] but it is remarkable that nonradiative decay is evidently very facile even at 10 K. It is not clear whether these processes are unimolecular or relate to some peculiarity of the (unknown) crystal structures of these two compounds.

Compound **5a** was unusual in that, while it displayed intense low-temperature luminescence similar to that of the first category discussed above, it had extremely weak room-temperature luminescence similar to that of the second category. A detailed study of the temperature dependence (Figure 5) was therefore undertaken. For temperatures above 80 K, both the emission intensity and lifetime follow the typical temperature dependence for a thermally activated nonradiative decay process.[21] An Arrhenius activation energy of ~2000 cm^{-1} can be fit to the data, but quantitative interpretation is made difficult by the fact that a simple low-temperature limit is not achieved. Indeed, the lifetime reaches a maximum value of 24.3 μs at 70 K (similar to a reported value of 18 μs at 77 K[22]) and then abruptly plummets over a range of less than 40 K to a value of 3.5 μs, which remains temperature independent over the range 10–30 K. This behavior is reproducible upon repeated recycling of the temperature for a given sample. The emission intensity undergoes similar but smaller changes over the 10–70 K temperature range.

Boltzmann-type unimolecular thermally activated processes cannot possibly account for such a huge decrease in emission lifetime as the temperature decreases, so it must represent some sort of cooperative phenomenon in the crystal.

It is evident that ^{3}LF excited states of Pt(α-diimine)X_2 complexes in the solid state exhibit a diverse variety of nonradiative decay mechanisms. We wish to emphasize that the spectral profiles of emission from these states are not diverse, instead

(20) Martin, M.; Krogh-Jespersen, M.-B.; Hsu, M.; Tewksbury, J.; Laurent, M.; Viswanath, K.; Patterson, H. *Inorg. Chem.* **1983**, *22*, 647.
(21) Bergkamp, M. A.; Watts, R. J.; Ford, P. C. *J. Phys. Chem.* **1981**, *85*, 684.
(22) Camassei, F. D.; Ancarani-Rossiello, L.; Castell, F. *J. Lumin.* **1973**, *8*, 71.

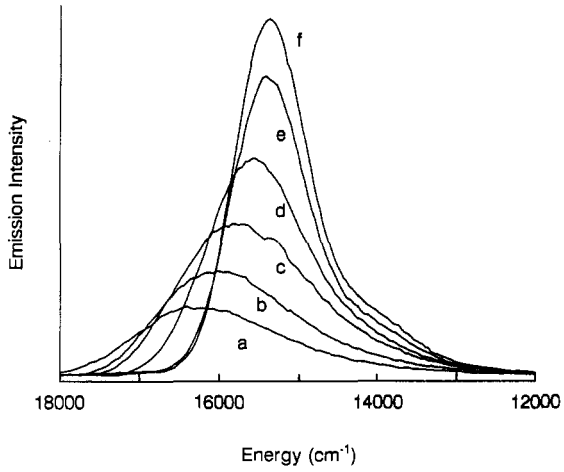

Figure 6. Emission spectra of solid **5b** as a function of temperature: (a) 300 K; (b) 200 K; (c) 150 K; (d) 100 K; (e) 50 K; (f) 10 K.

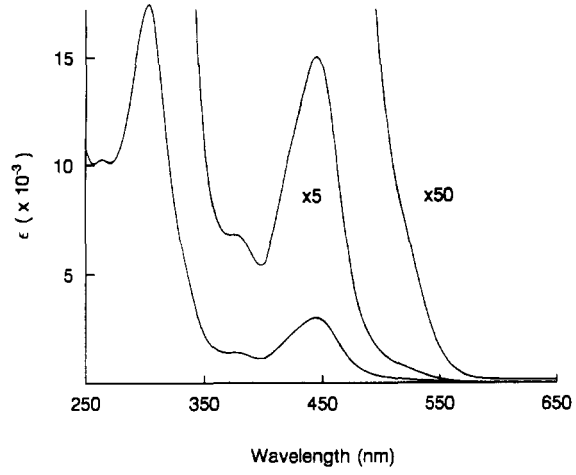

Figure 7. Room-temperature absorption spectrum of **8** in CH_2Cl_2 solution.

being highly characteristic of, and diagnostic for, lowest-energy ^{3}LF excited states.

Oligomer Emission. Compound **5b**, the red polymorph of Pt(bpy)Cl_2, has been shown[5b] to exhibit a linear-chain structure with a Pt–Pt distance of 3.45 Å. In this structure, the Pt(bpy)Cl_2 units have alternating orientations related by 180° rotation about the chain axis, so that there is no possibility for significant direct interaction between the bpy ligands of adjacent units. Thus, the red color, due to a strong absorption band[5a] at 19 600 cm^{-1}, must result in some way from the weak Pt–Pt interaction along the chains. The red form has recently been studied in detail at low temperatures by Gliemann et al.,[23] and we will discuss their work in detail below.

Emission spectra of **5b** as a function of temperature are shown in Figure 6. While the emission maximum for **5b** is similar to that of **5a**, the spectral profile is very different. Thus, the 300 K emission of **5b** is relatively narrow and asymmetric, and it drastically narrows and red-shifts as the temperature decreases. The large red shift is symptomatic of metal–metal involvement in the electronic transition, as the metal–metal distance typically exhibits [2b,18b] a large decrease in linear-chain compounds as the temperature decreases, owing to lattice contraction, and similar red shifts of electronic transitions have been documented[18b] in such cases. Furthermore, the 10 K emission spectrum shows resolution of a shoulder 1500 cm^{-1} to lower energy of the maximum. Vibronic structure in this vibrational interval indicates bpy distortion in the excited state. We note that the single-crystal absorption spectrum of **5b** at 10 K exhibits[23] its lowest energy resolved feature at 18 200 cm^{-1}, and this is strongly blue-shifted (~1000 cm^{-1}) at 300 K. Moreover, there is a weak absorption feature, identified as a vibronic sideband by Gliemann et al. because of its similar temperature dependence, about 1500 cm^{-1} to higher energy (band II of ref 23). The intensity of this feature relative to the absorption origin line is very similar to what we observe for the vibronic feature in emission (Figure 6).

In general, the data are all remarkably similar to those previously reported by us[2b,24] for the linear-chain compound Pt(bpy)$(CN)_2$ and related compounds. Thus, a similar assignment for the lowest energy, emissive excited state of **5b** can be made, ^{3}MLCT of the type $d\sigma^* \rightarrow \pi^*$(bpy), where $d\sigma^*$ is the filled Pt–Pt antibonding orbital derived from Pt(d_{z^2}) orbitals. We refer the reader to ref 2b for a more detailed discussion of this type of electronic transition.

Additional differences from ^{3}LF emission are evident in other photophysical properties. The emission lifetime increases monotonically and almost linearly as the temperature decreases to 10 K. (Data not shown. There is apparently a very large increase in lifetime at still lower temperatures, a value of 120 μs being reported for 1.6 K.[23] This low-temperature behavior is due to a small (15 cm^{-1}) spin–orbit splitting of the emissive triplet state.) The 300 K lifetime is much less than that of **2**, yet the emission intensities for these two compounds at room temperature are *roughly equal*.[25] Thus, the electronic transition involved in the emission of **5b** must be much more strongly allowed than that of **2**. This is typical of oligomeric Pt(II) MLCT emission[2b,c] versus (intrinsically weak) LF transitions.

It would appear that a linear-chain type structure is uncommon for Pt(α-diimine)X_2 (X = halide) compounds, and we have been unable to prepare polymorphs analogous to **5b** for **2**, **3**, **4**, **6**, and **7**. This situation contrasts with that for analogues with X = CN,[2b,24] for which linear-chain forms are common. Both steric and electronic factors may be involved in this difference.

Unimolecular MLCT. The compound Pt(bpy)Cl_2 has been shown[5a,26] to have its lowest energy ^{1}MLCT absorption at 25 400 cm^{-1} (ε 3400) in CH_2Cl_2 solution, and the maximum is very similar for crystalline **5a**.[5a] Evidently, ^{3}MLCT must lie above ^{3}LF for this compound, but the spacing of the states is clearly small enough that it should be possible to obtain related compounds for which ^{3}MLCT is the lowest energy excited state.

We achieved this aim with the dicarbomethoxy-substituted bpy derivative **8**. The electronic absorption spectrum is shown in Figure 7. The $^1(\pi\pi^*)$ absorption at 33 300 cm^{-1} (ε 17 700) is similar to that of **5**. The band at 22 500 cm^{-1} (ε 3030) is assigned to ^{1}MLCT, shifted 2900 cm^{-1} to lower energy from that of **5** by the electron-withdrawing carbomethoxy substituents on the bpy ligand. Additionally, a shoulder is observed at 19 000 cm^{-1} (ε 120), and we assign it to the transition to the corresponding ^{3}MLCT state. Our absorption spectrum is very similar to that reported in the literature.[9c]

Emission data for the solid compound are shown in Figure 8. The emission is clearly distinct from the ^{3}LF emissions presented earlier in that it has a highly asymmetric shape. The 300 K emission bears a mirror-image relationship to absorption, and there is good 0–0 overlap with the 19 000-cm^{-1} absorption shoulder. At 10 K, broad vibronic structure with a 1300-cm^{-1}

(23) Weiser-Wallfahrer, M.; Gliemann, G. *Z. Naturforsch.* **1990**, *45B*, 652.
(24) Che, C.-M.; Wan, K.-T.; He, L. Y.; Poon, C.-K.; Yam, V. W.-W. *J. Chem. Soc., Chem. Commun.* **1989**, 943.

(25) We estimated an emission quantum yield for solid **2** equal to 0.0063 at 300 K by the method of: Wrighton, M. S.; Ginley, D. S.; Morse, D. L. *J. Phys. Chem.* **1974**, *78*, 2229. The emission yield at 300 K for **5b** was determined to be 0.008 relative to **2** as a standard. The observed values of ϕ and τ imply radiative rate constants of 2×10^3 and 3×10^4 s^{-1} for **2** and **5b**, respectively.
(26) Gidney, P. M.; Gillard, R. D.; Heaton, B. T. *J. Chem. Soc., Dalton Trans.* **1973**, 132.
(27) Caspar, J. V.; Westmoreland, T. D.; Allen, G. H.; Bradley, P. G.; Meyer, T. J.; Woodruff, W. H. *J. Am. Chem. Soc.* **1984**, *106*, 3492 and references cited therein.

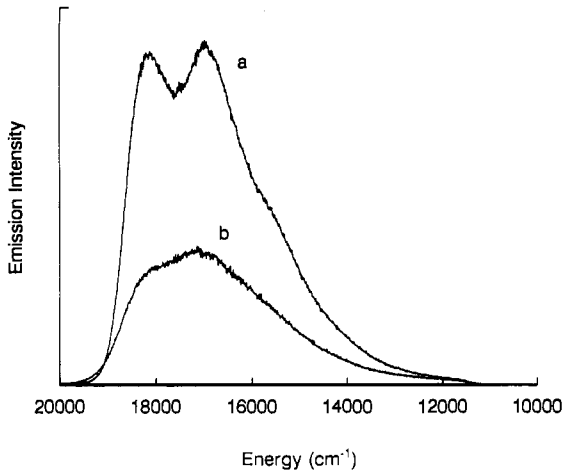

Figure 8. Emission spectra of solid **8** at 10 K (a) and 300 K (b). Excitation was at 457.9 nm.

spacing has developed. This is attributable to an "average" vibrational mode[28] of the substituted bpy ligand. The emission at 77 K of an ethanol/methanol glassy solution of the compound is very similar to the solid-state spectrum. The onset of low-temperature emission at about 18 700 cm^{-1} is taken to be the ^{3}MLCT 0–0 energy.

The shape of the emission, as well as the Huang–Rhys ratio (S; $I_{1,0}/I_{0,0}$) of about 1, is very similar to that of $Ru(bpy)_3^{2+}$ emission.[27] They may be contrasted to the sharper vibronic structure and larger S values characteristic of ^{3}IL emission.[2a]

That S (hence, excited-state α-diimine distortion) is larger for this unimolecular ^{3}MLCT emission than for the oligomer "metal–metal" ^{3}MLCT emission of **5b** deserves discussion. The likely explanation, consistent with the comparison to $Ru(bpy)_3^{2+}$, is that the excited state of **8** involves excitation from a π-bonding $d\pi(xz,yz)$ orbital. Excited-state distortion should therefore be larger than for **5b**, whose lowest MLCT state involves excitation from a $d\sigma^*$ (Pt–Pt) orbital derived from d_{z^2} orbitals that are formally π-nonbonding to bpy. Effects of this sort, involving changes in the degree of π-back-bonding interaction of d orbitals, have been previously invoked[27] to explain changes in S among various Ru and Os α-diimine complexes. There may also be increased mixing of the π^*(bpy) orbital with Pt p_z orbitals in the metal–metal-bonded case.

Regrettably, we find that **8** is nonemissive in CH_3CN or CH_2Cl_2 degassed solution at room temperature. While it would be grossly premature to generalize from one compound, it is possible that the coordinatively unsaturated, formally d^7 square-planar excited state may be subject to nonradiative deactivation in fluid solution via strong interaction with solvent, and/or non totally symmetric distortion; the short lifetimes of ^{3}LF states in fluid solution are attributable[28] to such effects.

Excited-State Energies. The energy of the $^3(\pi\pi^*)$ state of bpy coordinated to Pt(II) is well established from the $^3(\pi\pi^*)$ emission of the compound[2a] $[Pt(bpy)(en)](ClO_4)_2$. The onset of the sharply vibronically structured emission occurs at about 22 000 cm^{-1} at 77 K. Another estimate can be arrived at by splitting the difference between the lowest energy absorption and highest energy emission vibronic features (21 830 and 22 370 cm^{-1}, respectively) to give 22 100 cm^{-1}. Since the energies of the intense $^1(\pi\pi^*)$ absorption bands[2,21] (lowest energy vibronic feature at about 31 500 cm^{-1}) of $Pt(bpy)L_2^{n+}$ (L = halide, cyanide, amine) are insensitive to L, we assume that $^3(\pi\pi^*)$ is likewise insensitive, and $^3(\pi\pi^*)$ emissions[2a] for related compounds of the other α-diimine ligands of this study indicate very similar $^3(\pi\pi^*)$ energies.

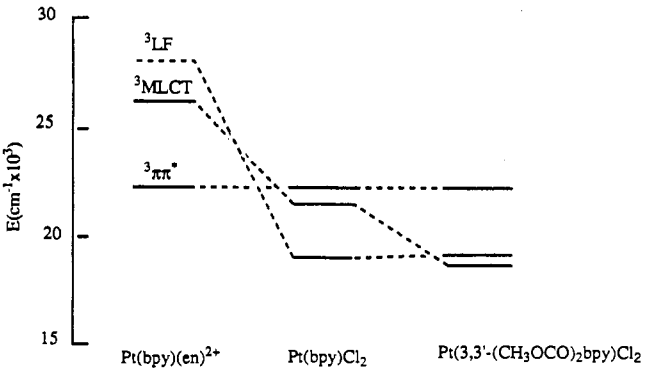

Figure 9. Estimates of the 0–0 energies of low-lying excited states of three Pt(II) bipyridine complexes.

It is more difficult to estimate the 0–0 energy of the LF transitions, particularly because the absorption bands, which are presumably very broad and weak,[29] are completely obscured by sharper and more intense MLCT and IL absorption bands. We obtain estimates in two ways. First, the 10 K ^{3}LF emissions of the Pt(α-diimine)Cl_2 complexes appear to reach zero intensity at about 19 000 cm^{-1}. This is a lower limit[30] for the 0–0 energy. Second, we use an equation proposed by Ford et al.[31] to estimate the 0–0 energy from the 10 K emission halfwidth and maximum, arriving at 18 900 cm^{-1}. The ^{3}LF energy of $Pt(bpy)(en)^{2+}$ cannot be directly estimated, but comparisons between compounds such as $Pt(NH_3)_4^{2+}$ and *cis*-$Pt(NH_3)_2Cl_2$ place[15] the ^{3}LF energy of the former about 5000–10 000 cm^{-1} to higher energy of the latter.

Finally, we attempt to estimate ^{3}MLCT energies. For **8** we found the ^{3}MLCT 0–0 energy (18 700 cm^{-1}) to lie 3700 cm^{-1} below the ^{1}MLCT absorption maximum of a room-temperature solution. The ^{1}MLCT solution absorption maxima of $[Pt(bpy)(en)]^{2+}$ (30 000 cm^{-1}, water solution[2a]) and **5** (25 400 cm^{-1}, CH_2Cl_2[5a,26]) then yield ^{3}MLCT estimates, assuming the same splitting, of about 26 300 and 21 700 cm^{-1}, respectively.

These estimates are summarized in Figure 9. The large stabilization of ^{3}MLCT for **5** can be attributed to the strongly electron-donating character of the chloride ligands. The fact that ^{1}MLCT lies at very similar energies for[2a] $[Pt(bpy)(en)]^{2+}$ and[24] $Pt(bpy)(CN)_2$ suggests a special role for the π-donor capacity of chloride, and support for this idea comes from the fact that ^{1}MLCT is further red-shifted to 23 700 cm^{-1} for **7** in CH_2Cl_2 solution. However, it is known that extremely strong σ-donors such as methyl likewise produce greatly stabilized MLCT states for compounds such as $Pt(bpy)(CH_3)_2$.[32] In any case, it is evident that stabilization of the α-diimine MLCT states by ancillary halide ligands is sufficiently large that they may conceivably drop below ^{3}IL states and might therefore be the lowest energy excited states if ^{3}LF excited states were not still more stabilized by the weak-field halide ligands. A plausible approach to achieving ^{3}MLCT as the lowest energy excited state (other than the one employed in the present work of substituting the α-diimine ligand with electron-withdrawing substituents) would be to replace halide with strongly electron-donating but *strong*-field ancillary ligands such as CH_3, and this approach is currently being investigated by us.

Finally, we note that the onset of 10 K emission of **5b** at about 16 500 cm^{-1} places this metal–metal MLCT excited state well below our estimate of the ^{3}LF energy. The LF excited states involving d_{z^2} excitation should include $d\sigma^* \rightarrow x^2-y^2$ components that are stabilized relative to monomer states,[33] much like the

(28) (a) Moggi, L.; Varani, G.; Sabbatini, N.; Balzani, V. *Mol. Photochem.* **1971**, *3*, 141. (b) Bolletta, F.; Gleria, M.; Balzani, V. *J. Phys. Chem.* **1972**, *76*, 3934.

(29) The lowest energy ^{3}LF absorption band of *cis*-$Pt(NH_3)_2Cl_2$ has been assigned[12] to a weak MCD feature at 23,700 cm^{-1}.

(30) Miskowski, V. M.; Gray, H. B.; Wilson, R. B.; Solomon, E. I. *Inorg. Chem.* **1979**, *18*, 1410.

(31) Petersen, J. D.; Watts, R. J.; Ford, P. C. *J. Am. Chem. Soc.* **1976**, *98*, 3188.

(32) Chaudhury, N.; Puddephatt, R. J. *J. Organomet. Chem.* **1975**, *84*, 105.

involving d_{z^2} excitation should include $d\sigma^* \rightarrow x^2 - y^2$ components that are stabilized relative to monomer states,[33] much like the MLCT states. Assignments for *cis*-$Pt(NH_3)_2Cl_2$,[12] however, place the monomer $z^2 \rightarrow x^2 - y^2$ excitation as the highest energy d–d one (see also ref 15 for discussion of the LF state ordering). Thus, even if this type of LF state is considerably stabilized by metal–metal interaction, it need not necessarily drop below the metal–metal-stabilized MLCT state.

(33) Stiegman, A. E.; Rice, S. F.; Gray, H. B.; Miskowski, V. M. *Inorg. Chem.* **1987**, *26*, 1112.

Acknowledgment. V.M.M. and V.H.H. thank Bill Connick, Jim Bailey, and Harry Gray for many helpful discussions. C.-M.C. acknowledges the Hong Kong Research Grant Council for financial support and the National Taiwan University for a visiting professorship. This work at Caltech was supported by the Office of Naval Research.

Supplementary Material Available: Figure S-1, showing the unit cell packing diagram for compound **6**, and Tables S-I–S-IV, giving positional and thermal parameters for the structures of **6** and **8** (4 pages). Ordering information is given on any current masthead page.